nanomaterials

MDPI

Article

Liposomal Nanoformulation as a Carrier for Curcumin and pEGCG—Study on Stability and Anticancer Potential

Ludwika Piwowarczyk [1,*], Malgorzata Kucinska [2], Szymon Tomczak [1], Dariusz T. Mlynarczyk [3], Jaroslaw Piskorz [4], Tomasz Goslinski [3], Marek Murias [2] and Anna Jelinska [1]

[1] Chair and Department of Pharmaceutical Chemistry, Poznan University of Medical Sciences, Grunwaldzka 6, 60-780 Poznan, Poland; szymon.tomczak@ump.edu.pl (S.T.); ajelinsk@ump.edu.pl (A.J.)
[2] Chair and Department of Toxicology, Poznan University of Medical Sciences, Dojazd 30, 60-631 Poznan, Poland; kucinska@ump.edu.pl (M.K.); marek.murias@ump.edu.pl (M.M.)
[3] Chair and Department of Chemical Technology of Drugs, Poznan University of Medical Sciences, Grunwaldzka 6, 60-780 Poznan, Poland; mlynarczykd@ump.edu.pl (D.T.M.); tomasz.goslinski@ump.edu.pl (T.G.)
[4] Chair and Department of Inorganic & Analytical Chemistry, Poznan University of Medical Sciences, Grunwaldzka 6, 60-780 Poznan, Poland; piskorzj@ump.edu.pl
* Correspondence: ludwika.piwowarczyk@wp.eu; Tel.: +48-61-854-6617

Abstract: Nanoformulations are regarded as a promising tool to enable the efficient delivery of active pharmaceutical ingredients to the target site. One of the best-known and most studied nanoformulations are liposomes—spherical phospholipid bilayered nanocarriers resembling cell membranes. In order to assess the possible effect of a mixture of polyphenols on both the stability of the formulation and its biological activity, two compounds were embedded in the liposomes—(i) curcumin (CUR), (ii) a peracetylated derivative of (−)-epigallocatechin 3-*O*-gallate (pEGCG), and (iii) a combination of the aforementioned. The stability of the formulations was assessed in two different temperature ranges (4–8 and 20 °C) by monitoring both the particle size and their concentration. It was found that after 28 days of the experiment, the liposomes remained largely unchanged in terms of the particle size distribution, with the greatest change from 130 to 146 nm. The potential decomposition of the carried substances was evaluated using HPLC. The combined CUR and pEGCG was sensitive to temperature conditions; however its stability was greatly increased when compared to the solutions of the individual compounds alone—up to 9.67% of the initial concentration of pEGCG in liposomes after 28 days storage compared to complete decomposition within hours for the non-encapsulated sample. The potential of the prepared formulations was assessed in vitro on prostate (LNCaP) and bladder cancer (5637) cell lines, as well as on a non-cancerous human lung fibroblast cell line (MRC-5), with the highest activity of IC_{50} equal 15.33 ± 2.03 µm for the mixture of compounds towards the 5637 cell line.

Keywords: bladder cancer; curcumin; epigallocatechin gallate; liposomes; prostate cancer; stability

Citation: Piwowarczyk, L.; Kucinska, M.; Tomczak, S.; Mlynarczyk, D.T.; Piskorz, J.; Goslinski, T.; Murias, M.; Jelinska, A. Liposomal Nanoformulation as a Carrier for Curcumin and pEGCG—Study on Stability and Anticancer Potential. *Nanomaterials* **2022**, *12*, 1274. https://doi.org/10.3390/nano12081274

Academic Editor: Abdelhamid Elaissari

Received: 25 February 2022
Accepted: 5 April 2022
Published: 8 April 2022

1. Introduction

Cancers of the urogenital system include, among others, prostate cancer and bladder cancer (BC) [1]. The urinary bladder is a hollow organ of muscle tissue located in the lower abdomen behind the symphysis pubis. Bladder cancer is a heterogeneous disease and is a spectrum of lesions of varying degrees of malignancy, infiltration depth, and disease progression risk. BC is the tenth most common cancer globally, and its incidence continues to increase worldwide. The increased risk of developing bladder cancer is more common in heavy smokers and also in men than in women. Southern Europe is one of the regions with the highest incidence of bladder cancer, with 26.5/100 000 men and 5.5/100 000 women each year developing the disease. Other factors include exposure

to carcinogens (e.g., aromatic amines), *Schistosoma haematobium* infection, past bladder irradiation, prolonged and recurrent cystitis, and long-term use of a bladder catheter [2–4].

There are non-muscle-invasive (NMIBC) and muscle-invasive tumors (MIBC) in BC. Patients with confirmed bladder cancer are classified by tumor grade and by tumor stage, according to the recently published American Joint Committee on Cancer (AJCC). Moreover, BC treatment is dependent on the tumor-node-metastasis(TNM) staging system (Ta, Tis, T1–T4) and other factors like the patient's overall condition and age, and the tolerability of the treatment method [5,6]. The type of NMIBC is treated with transurethral resection, most commonly followed by immunotherapy using the Bacillus Calmette-Guérin (BCG) vaccine or intravesical chemotherapy. In contrast, MIBC is usually treated with radical cystectomy and neoadjuvant chemotherapy due to higher rates of progression and relapse [7]. The administration of standard chemotherapeutic drugs causes many side effects, while immunotherapy can cause local irritation of the bladder epithelium. Relapses of the disease are frequent and require repeated resections, and therefore, it is desirable to look for new treatment options to prevent such relapses and metastasis [8]. The prostate is a single muscle-glandular organ, which is part of the male reproductive system. Prostate cancer was among the most common cancers diagnosed in men in the United States in 2017. The therapeutic potential of prostate cancer has improved significantly in recent years, although, it is still necessary to search for new drugs, especially in patients with advanced forms of the disease [9].

Polyphenols constitute a large and diverse group of organic compounds characterized by hydroxyl groups attached to an aromatic ring. Various studies indicate that the consumption of polyphenols may play an essential role in the regulation of the metabolism, as well as chronic and neoplastic disease treatment. At present, more than 8 000 polyphenols have been identified, but their impact on human health is not yet fully understood [10]. (−)-Epigallocatechin-3-*O*-gallate (EGCG) is a polyphenol found in abundance in green tea (*Camellia sinensis*) leaves, which exhibits pleiotropic biological activity, including anti-inflammatory and anticancer effects [11]. The most significant obstacles to the widespread use of this compound are its low oral bioavailability and also its chemical instability, which is induced by two major processes, epimerization, and auto-oxidation (in phosphate-buffered saline—60 mM, pH 7.4—at 37 °C, the stability of EGCG is only 1.5 h) [12].

Curcumin (CUR) is a polyphenolic compound with characteristic yellow color, obtained by extracting turmeric rhizomes (*Curcuma longa*), and consisting of two feruloyl residues linked by a methylene group. It has antioxidant, anti-inflammatory, antibacterial, and antiviral properties, as well as having shown to have potent anti-cancer activity. It is a promising drug candidate in liver and kidney disease, diabetes, cardiovascular diseases, arthritis, psoriasis, and neurodegenerative diseases, such as Alzheimer's. It is also noteworthy that it is safe in large doses up to 12 g/24 h. The main factors limiting the use of curcumin is its low bioavailability, instability under physiological conditions, poor absorption from the gastrointestinal tract, and rapid metabolism [13–16], although these can be overcome with the use of nanoformulations. Nanoformulations allow precise drug delivery using nanoparticles, which can increase the biological activity of CUR and its targeting to previously inaccessible sites [17]. Research also indicates an improvement in the solubility of nanocurcumin and optimized intracellular uptake.

To date, liposomes are among the most popular nanoparticles for curcumin delivery [18]. Liposomes are spherical vesicles with a hydrophilic core encircled by phospholipid layers and are classified according to their size: small, large, and giant vesicles; number of layers: single, oligo- and multilayered; and phospholipid charge: neutral, anionic, or cationic [19].They are mainly composed of natural and/or synthetic phospholipids with amphipathic properties, a characteristic feature of which is spontaneously aggregating at the phase boundary [20]. Liposomes as drug nanocarriers provide enormous possibility for modifying physicochemical and structural properties, which features could significantly influence the drug distribution in vivo, e.g., its stability, adequate drug release, biodistri-

bution, and cellular uptake of the liposomes [21]. Moreover, by protecting the medicinal substances through encapsulation in liposomes it is possible to prevent degradation [22].

Herein, we present research on the possibility of encapsulating selected polyphenols (CUR and pEGCG) in liposomal carriers for drug delivery and combining substances to provide an advantage in anticancer potential towards urogenital cancer cell lines. Moreover, we demonstrate the methodology of preparing liposomal formulation by co-embedding two active substances, thus enhancing the time-dependent stability of compounds enclosed in those nanocarriers. The structures of the compounds used in the current study are presented in Figure 1.

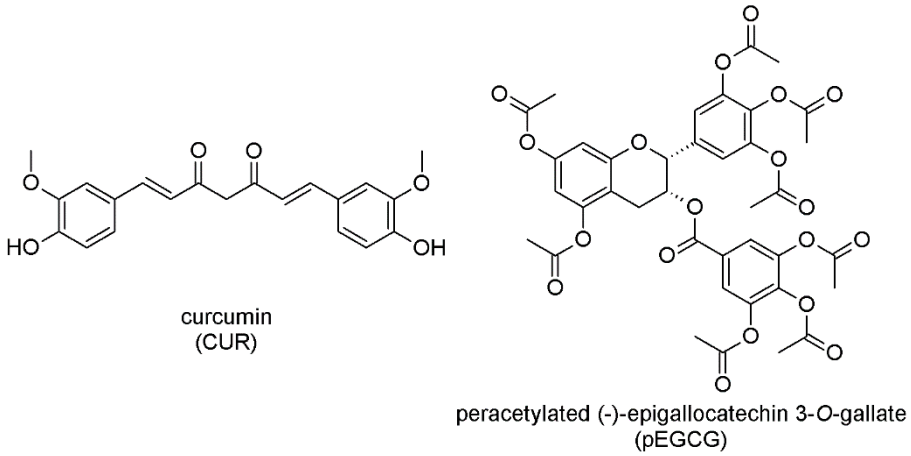

Figure 1. Chemical structures of curcumin ((1E,6E)-1,7-bis(4-hydroxy-3-methoxyphenyl)hepta-1,6-diene-3,5-dione; CUR) and peracetylated EGCG (3′,3″,4, 4″, 5, 5″,7-*O*-octaacetyl-(−)-epigallocatechin 3-*O*-gallate; pEGCG).

2. Materials and Methods

2.1. Chemical Compounds and Reagents

Curcumin, (1E,6E)-1,7-bis(4-hydroxy-3-methoxyphenyl)hepta-1,6-diene-3,5-dione, was obtained from Fluorochem (Derbyshire, United Kingdom). 1-Palmitoyl-2-oleoyl-glycero-3-phosphocholine (POPC) and 1,2-dioleoyl-3-trimethylammonium-propane (DOTAP) were obtained from Avanti Polar Lipids (Birmingham, AL, USA).

HPLC grade acetonitrile, water, acetic acid and potassium chloride were procured from Avantor Performance Materials (Gliwice, Poland).

The peracetylated derivative of EGCG, 3′,3″,4′,4″,5,5′,5″,7-*O*-octaacetyl-(–)-epigallocatechin 3-*O*-gallate, was prepared according to a literature procedure [23].

Reagents used for in vitro experiments, such as fetal bovine serum (FBS), phosphate-buffered saline (PBS), trypsin-EDTA, L-glutamine, dimethylsulfoxide (DMSO), 3-(4,5-dimethylthiazol-2-yl)-2,5-diphenyltetrazolium bromide (MTT), were obtained from Sigma Aldrich (St. Louis, MO, USA). The DMSO for dissolving formazan crystals was obtained from Avantor Performance Materials (Gliwice, Poland). The following cell lines: 5637 (human bladder grade II carcinoma), LNCaP (human prostate carcinoma), and non-cancerous cell line MRC-5 (normal human lung fibroblast) were purchased from the American Type Culture Collection (ATCC, Manassas, VA, USA). The LNCaP and MRC-5 cell lines were maintained in DMEM medium, and 5637 in RPMI-1640 supplemented with 10% (*v*/*v*) FBS, 1% (*v*/*v*) L-glutamine (200 mM), 1% (*v*/*v*), 10 000 penicillin units, 10 mg/mL streptomycin solution. Cells were cultured at 37 °C, 5% CO_2, and 95% humidity atmosphere.

2.2. Liposome Preparation

A modified thin-film hydration method was used to embed compounds in the liposomal formulation [24]. A schematic illustration of the preparation of liposomes via thin-film hydration is presented in Figure 2. Liposomes were prepared from 1-palmitoyl-2-oleoyl-sn-

glycero-3-phosphocholine (POPC) or POPC/1,2-dioleoyl-3-trimethylammonium-propane (DOTAP) mixture (9:1 or 8:2), and either CUR, pEGCG, or their combination with a molar ratio of 1.7:10 (CUR:lipids), 1.7:10 (pEGCG:lipids), and 0.8:0.8:10 (CUR:pEGCG:lipids). The final concentrations were as follows: 614.0 µg/mL CUR, 1 324.4 µg/mL pEGCG, 7 600.8 µg/mL POPC and 307.0 + 662.2 µg/mL mixture of compounds (CUR+pEGCG). Briefly, the lipids and chemical compounds were dissolved in chloroform in the specified molar ratio, the solvent was evaporated, and the resulting film dried in a vacuum (15 min). After that, it was rehydrated using PBS, vortexed, and sonicated in an ultrasonic bath (5 min/180 W) until the uniform suspension was achieved. Next, the particle size was unified using Avanti® Polar Lipids Mini Extruder (Merck KGaA, Darmstadt, Germany) with 100 nm polycarbonate membranes, according to the manufacturer's instructions.

The encapsulation efficiency (EE) of CUR, pEGCG and their mixture was calculated according to the formula [25]:

$$EE = C_{en}/C_{in} \times 100\%$$

where C_{en}—the actual amount of the substance in the liposomes measured after their disruption using HPLC, C_{in}—the initial amount of the substance used for the preparation of the liposomes.

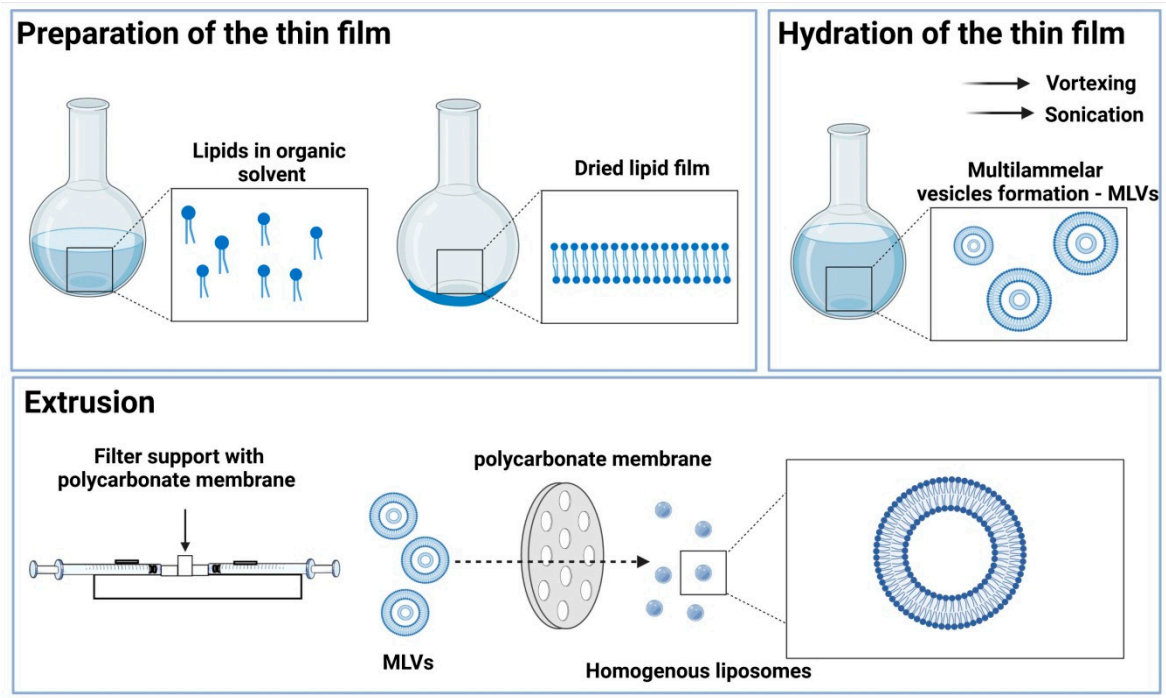

Figure 2. The schematic illustration of liposomes preparation protocol using the thin-film hydration followed by extrusion method. The image was prepared according to Zhang [26] and created with *BioRender.com* and Servier Medical Art (last accessed on 10 January 2022).

2.3. Liposome Size and Zeta Potential Measurement

Liposome size was determined in PBS buffer using Nanoparticle Tracking Analysis (NTA) technique on a Nanosight LM10, equipped with a sCMOS camera and 405 nm laser, with NTA 3.2 Dev Build 3.2.16 software (Malvern Panalytical, Malvern, UK). This equipment analyzes videos captured using the instrument, giving a particle size distribution and particle count based upon tracking each particle's Brownian motion and the size being calculated according to the Stokes-Einstein equation [27,28]. The samples of the liposomes were diluted 1:10 000 to achieve the concentration operating range of the equipment [29]. Zeta potential was measured using Zetasizer Nano ZS (Malvern Instruments, Malvern,

UK). Measurements were performed in triplicate. 100 µL of liposomes were diluted with 10 mL of water.

2.4. HPLC Analysis

The stability studies were carried out using the HPLC method, validated for selectivity, precision, and linearity. The applied method met the accepted validation criteria. The method was developed to determine the concentration of CUR and pEGCG. The analytical apparatus comprised a 1220 Infinity LC chromatography system (Agilent Technologies, Santa Clara, CA, USA) equipped with a DAD detector, a G1315C optical unit, an autosampler, and a column oven. The gradient elution utilizes the mobile phase consisting of acetonitrile (phase A) and 1% acetic acid solution with potassium chloride (2 g/1 L, phase B) ratio 5%/95% at 0 min. Mobile phase concentration changed to 100%/0%, A/B in 30 min and returned to the starting ratio within 10 min (40 min). The stationary phase was octadecylsilyl silica gel for chromatography (Lichrospher® 100 RP-18 column, 25 × 4 mm; 5 µm, Merck), stored at 25 ± 1 °C. The UV wavelength, flow rate and injection volume were 280 nm, 1.05 mL/min, and 20 µL, respectively. The retention time for CUR was 20.7 min, for pEGCG—22.0 min, and the analysis run time was 40 min. Each sample was injected in triplicate. The validation of the HPLC method concerned selectivity, precision, linearity, range, and limits of detection and quantitation was performed.

2.5. Biological Activity Assessment

The cytotoxic effect of the tested formulations was determined using the MTT assay [30,31], with some modifications [32]. 5637 and MRC-5 cells were seeded at a density of 15 × 10^3 cells/well, while LNCaP cells were seeded at a density of 10 × 10^3 cells/well in 96-well plates, and incubated overnight. The cells were treated with pEGCG and CUR (dissolved in DMSO) at the concentration of 3, 6, 12, 25, 50 and 100 µm. The DMSO was used as a control, and its concentration in the medium did not exceed 0.1%. For testing of the liposomal formulations, the tested compounds were added at a concentration of 1.2, 2.5, 5, 10, 20, and 40 µm. The combination of both compounds was tested at a concentration of 0.6, 1.2, 2.5, 5, 10, and 20 µm. The two controls were used: cell culture medium and empty liposomes (at a concentration corresponding to the higher tested dose).

The MTT assay was performed after 24 and 48 h. Briefly, the cells were washed twice with PBS, and MTT (0.59 mg/mL) was then added to each well, and incubated for 1.5 h at standard cell culture conditions. The formazan crystals were dissolved in 200 µL of DMSO, and the absorbance was measured at 570 nm with a plate reader (Biotek Instruments, Elx-800, Winooski, VT, USA). Cell viability was calculated as a percentage of the control (cell culture medium for liposomal formulation, and DMSO in cell culture medium for free form). All experiments were repeated at least three times (only pEGCG toxicity against 5637 cells was determined from two independent experiments). The IC_{50} values were determined using GraphPad 8.0 software.

2.6. Statistical Analysis

The statistical analysis was performed using GraphPad Prism®8 (GraphPad Software, Inc., La Jolla, CA, USA). One-way ANOVA with post-hoc Tukey's test and Dunnett's test were used to determine the significance; $p < 0.05$ was considered significant.

3. Results and Discussion

The rationale for including two polyphenols together in an formulation was to assess whether the individual components, which already exhibited anticancer activity, would interact to improve formulation stability, encapsulation efficiency, and reveal a synergistic effect [33–36].

Due to the instability of EGCG [12], the fully acetylated derivative of (−)-epigallocatechin 3-gallate (pEGCG) was used instead of the most commonly studied EGCG. The liposomes were prepared by a modified thin-film hydration method. The concentration of curcumin

and peracetylated EGCG within the liposomes was established experimentally as both compounds reveal low biological activity. In order to achieve the desired anti-cancer effect, high concentrations in lipids were used [37], which allowed the extrusion of further resulting liposomes. Such concentration was found to be at 1 666 µm and the encapsulation efficiency was: 92.26 ± 1.19% for CUR, 54.58 ± 9.71% for pEGCG, and 91.51 ± 1.62% for CUR from the mixture (CUR+pEGCG) and 76.84 ± 0.61% of pEGCG from the mixture (CUR+pEGCG). Preparing liposomes containing higher concentrations of CUR or pEGCG resulted in too high resistance during the mechanical unification of the liposome size, which in turn caused either leaks from the equipment and subsequent loss of the formulation dispersion, or perforation of the polycarbonate membranes. The concentration of the curcumin causing disturbances in the liposomes was reported at 60 mg/L (~163 µm). This was because the lipid applied was dioleoylphosphatidylcholine, which formed smaller liposomes (65 nm) [38]. Interestingly, Wu et al. reported that the encapsulation efficiency of curcumin in the liposomes might either increase or decrease along with the increasing ratio of CUR to lipid ratio, depending on the type of phospholipids used [39].

3.1. Liposome Size

The liposomes were studied in terms of their particle size to ensure the efficiency and repeatability of the obtained biological results. The size of the liposomes was measured immediately before the in vitro test, and the results are presented in Figure 3 and Table 1. The mean particle size of the prepared liposomes was about 100 nm, which is essential to increase biodistribution in potential subsequent in vivo activity studies [40,41]. In general, the particle size analyses of liposomal formulations were performed using Dynamic Light Scattering (DLS; data not shown) and NTA, while the zeta potential was determined using Electrophoretic Light Scattering (ELS) available in the Zetasizer Nano device. It should be noted that during NTA, size distribution and nanoparticle concentration are measured in real-time; thus allowing the early detection of physical instability, otherwise indeterminable if the changes in size distribution are minimal [42].

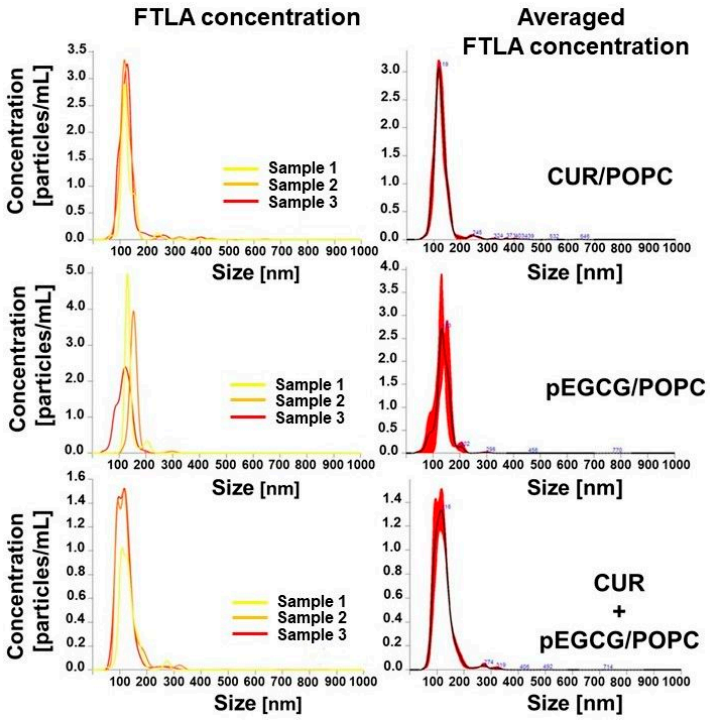

Figure 3. The mean hydrodynamic diameter distribution patterns of the prepared liposomes subjected to biological evaluation. FTLA—the finite track length adjustment.

Table 1. The size of the liposomes and their concentration as prepared immediately before the biological activity study.

Compound	Particle Size (±SD) [nm]	PDI [a]	Concentration (±SD) [Particles/mL]
CUR	129.9 ± 45.0	0.120	$1.48 \times 10^{13} \pm 1.87 \times 10^{12}$
pEGCG	136.8 ± 33.5	0.060	$1.39 \times 10^{13} \pm 8.47 \times 10^{11}$
CUR+pEGCG	123.3 ± 41.8	0.115	$8.89 \times 10^{12} \pm 1.29 \times 10^{12}$

[a]—polydispersity index calculated according to the formula PDI = (SD/particle size)^2 [43].

Zeta potential provides information about the surface charge properties of a nanoparticle, which can present cationic, anionic, or neutral character. According to the interpretation of the zeta potential, the values in the range of −10 to +10 mV are considered to be neutral for liposomes. Zeta potential measurements provide information about the ion concentration in the immediate vicinity of the membrane. Moreover, the magnitude of the zeta potential indicates the stability of colloidal systems [44]. In the herein presented study, zeta potential values ranged from −7.04 (pEGCG) to −4.76 (CUR) mV, which confirms the neutral character of obtained liposomes.

3.2. Liposomal Formulation Stability Study

3.2.1. Particle Size and Particle Concentration

The particle size and concentration of the prepared liposomes were monitored throughout 28 days of the storage experiment. The EGCG or CUR-containing liposomes were kept in the refrigerator (at 4–8 °C) or at room temperature (20 °C). The results of the study are presented in Table 2 and Figure 4.

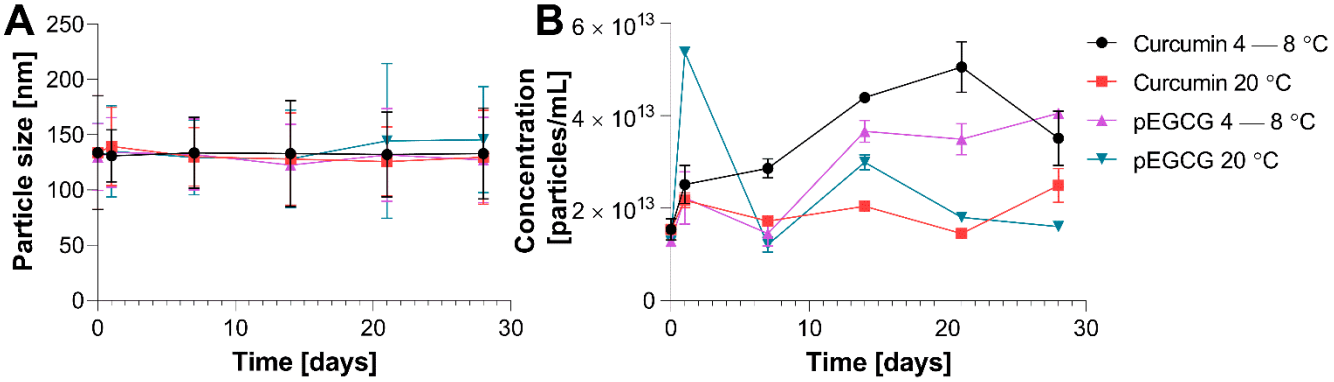

Figure 4. (**A**) the change of the mean liposome size over 28 days of experiment depending on the storage conditions; (**B**) the change of the mean liposome concentration over 28 days of experiment depending on the storage conditions. Error bars represent standard deviation of the mean.

The mean particle size of the prepared liposomes exceeded 100 nm, even though they were extruded through 100 nm carbonate filters. A possible reason for this is that upon extrusion, the liposomes could have disassembled and assembled. Another possible reason could be because of the methodology of the particle size measurement—the obtained values are for hydrodynamic diameters calculated in solution, so there might be an interaction between the solvent (water) and the liposome surface resulting in the formation of solvation (hydration) shell [45].

Table 2. The size of the liposomes and their concentration depending on the storage conditions and embedded polyphenol.

Temperature	Curcumin			
	Storage Time [Days]	Particle Size (±SD) [nm]	PDI [a]	Concentration (±SD) [Particles/mL]
4–8 °C	0	133.8 ± 51.5	0.148	$1.54 \times 10^{13} \pm 2.31 \times 10^{12}$
	1	130.9 ± 23.6	0.033	$2.51 \times 10^{13} \pm 4.11 \times 10^{12}$
	7	133.6 ± 32.2	0.058	$2.86 \times 10^{13} \pm 2.07 \times 10^{12}$
	14	133.0 ± 48.0	0.130	$4.39 \times 10^{13} \pm 1.04 \times 10^{12}$
	21	132.1 ± 38.4	0.085	$5.05 \times 10^{13} \pm 5.45 \times 10^{12}$
	28	133.1 ± 41.1	0.095	$3.51 \times 10^{13} \pm 5.87 \times 10^{12}$
20 °C	1	139.4 ± 35.5	0.065	$2.17 \times 10^{13} \pm 1.63 \times 10^{12}$
	7	130.1 ± 26.5	0.041	$1.72 \times 10^{13} \pm 2.44 \times 10^{11}$
	14	128.0 ± 41.6	0.106	$2.04 \times 10^{13} \pm 8.49 \times 10^{11}$
	21	125.8 ± 31.3	0.062	$1.45 \times 10^{13} \pm 4.75 \times 10^{11}$
	28	129.7 ± 42.5	0.107	$2.49 \times 10^{13} \pm 3.66 \times 10^{12}$
Temperature	pEGCG			
	Storage Time [Days]	Particle Size (±SD) [nm]	PDI [a]	Concentration (±SD) [Particles/mL]
4–8 °C	0	129.8 ± 30.3	0.054	$1.28 \times 10^{13} \pm 8.67 \times 10^{11}$
	1	134.0 ± 31.6	0.056	$2.22 \times 10^{13} \pm 5.67 \times 10^{12}$
	7	132.2 ± 32.0	0.059	$1.45 \times 10^{13} \pm 2.73 \times 10^{12}$
	14	122.7 ± 36.9	0.090	$3.66 \times 10^{13} \pm 2.39 \times 10^{12}$
	21	131.7 ± 41.9	0.101	$3.49 \times 10^{13} \pm 3.37 \times 10^{12}$
	28	127.2 ± 38.6	0.092	$4.05 \times 10^{13} \pm 9.78 \times 10^{11}$
20 °C	1	135.1 ± 41.2	0.093	$5.37 \times 10^{13} \pm 5.03 \times 10^{11}$
	7	129.5 ± 33.7	0.068	$1.21 \times 10^{13} \pm 1.60 \times 10^{12}$
	14	128.2 ± 44.2	0.119	$2.99 \times 10^{13} \pm 1.62 \times 10^{12}$
	21	144.4 ± 70.1	0.236	$1.80 \times 10^{13} \pm 4.22 \times 10^{11}$
	28	145.6 ± 48.0	0.109	$1.60 \times 10^{13} \pm 1.04 \times 10^{12}$

[a]—polydispersity index calculated according to the formula PDI = (SD/particle size)^2 [43].

The increase in the liposome size over time may be due to the agglomeration of liposomes or even the merging of liposomes with each other. If multilamellar vesicles are formed, several phenomena might appear. Firstly, the layers might merge, leading to the formation of less-layered larger liposomes, which in turn may disassemble and reassemble, therefore yielding more liposomes. Another alternative is that the outer layer may detach from the liposomes and merge with another liposome thus increasing its size, and form a liposome by itself or assemble with another group of phospholipids to form a new vesicle. What can also occur is that the water trapped between the liposome layers may be expelled, leading to smaller-size liposomes [46].

The values of the polydispersity index (PDI) obtained for the prepared CUR and pEGCG loaded liposomes are less than 0.15 (except for one measurement for pEGCG on day 21 at room temperature, for which the PDI is 0.23). The FDA mentions the importance of the uniform distribution of the liposome size in its guidelines; however, there is no threshold value stated. Based on the literature data on the subject, if the PDI value does not exceed 0.3, the obtained liposome suspension is regarded as homogeneous [47,48]. Therefore, the obtained liposome mixtures are characterized by a homogeneous vesicle size distribution.

3.2.2. Stability Study at Room (20 °C) and Refrigerator (4–8 °C) Temperatures

Unexpectedly, the concentration of the curcumin in CUR/POPC showed a greater decrease when stored in the range 4–8 °C (41% of the initial value) than at the room temperature (58%). Usually, the decomposition of CUR in liposomes is faster when

the temperature is higher [46]. This might be due to the increase of rigidity of lipids at a lower temperature which in turn provides easier access of CUR to water. In the case of CUR in CUR/pEGCG/POPC formulation, there was almost no difference in the concentration changes between the experiments conducted at different temperatures (Figure 5, Tables 3 and 4). However, CUR was more stable at the refrigerator temperature in CUR+pEGCG/POPC formulation than in the CUR/POPC formulation. This might suggest that pEGCG induced a protective effect on CUR when co-embedded in the liposomes, as both exhibit highly lipophilic character and are placed in the lipid layer of the liposomes. A similar phenomenon for CUR and resveratrol has been reported [49].

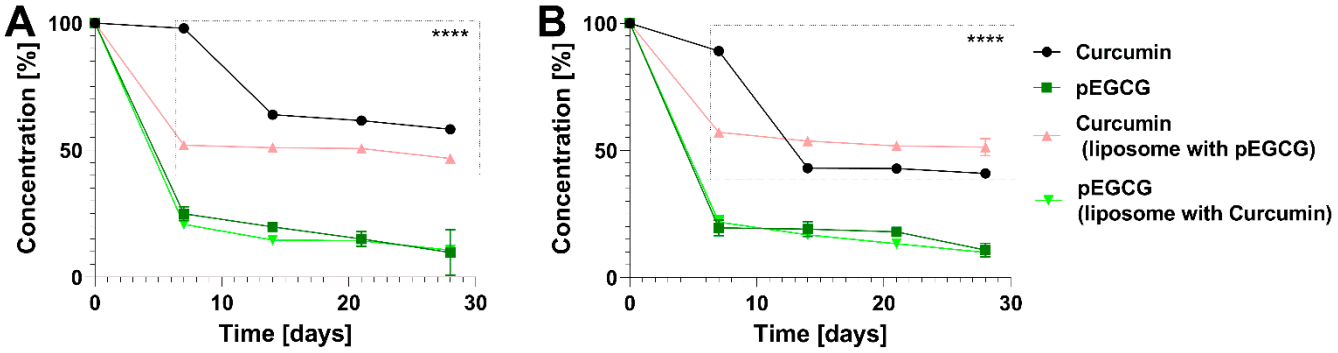

Figure 5. Stability study of CUR, pEGCG and their combination in liposomal nanoformulations at: (**A**) room temperature (20 °C), and (**B**) refrigerator temperature (4–8 °C). Statistical significance was assessed by Tukey's Test (**** $p < 0.0001$). Error bars represent standard deviations of the mean.

Table 3. Changes in the concentration of CUR and pEGCG in liposomal nanoformulations in the stability study in room temperature (20 °C).

Time [Days]	CUR C/C_0	SD	pEGCG C/C_0	SD	CUR C/C_0 (CUR+pEGCG)	SD	pEGCG C/C_0 (CUR+pEGCG)	SD
0	100.00%	0.18%	100.00%	0.84%	100.00%	0.61%	100.00%	1.58%
7	97.93%	0.61%	24.98%	2.81%	51.96%	0.62%	20.76%	0.38%
14	63.92%	1.35%	19.82%	0.26%	50.95%	0.50%	14.64%	0.46%
21	61.64%	0.05%	15.03%	2.89%	50.65%	1.37%	14.30%	0.00%
28	58.21%	0.90%	9.67%	9.01%	46.67%	0.72%	10.65%	0.47%

C/C_0 is the ratio between the concentration tested at a certain time point to the initial concentration at the beginning of the experiment. SD—standard deviation.

Table 4. Changes in the concentration of CUR and pEGCG in liposomal nanoformulations in the stability study at refrigerator temperature (4–8 °C).

Time [Days]	CUR C/C_0	SD	pEGCG C/C_0	SD	CUR C/C_0 (CUR+pEGCG)	SD	pEGCG C/C_0 (CUR+pEGCG)	SD
0	100.00%	0.18%	100.00%	0.84%	100.00%	0.61%	100.00%	1.58%
7	89.16%	1.48%	19.58%	3.09%	57.15%	0.18%	21.81%	2.52%
14	43.00%	0.09%	19.07%	2.93%	53.67%	0.03%	16.82%	0.10%
21	42.84%	1.09%	17.98%	0.86%	51.81%	0.31%	13.27%	1.13%
28	40.94%	1.06%	10.77%	2.72%	51.27%	3.38%	9.87%	0.34%

C/C_0 is the ratio between the concentration tested at a certain timepoint to the initial concentration at the beginning of the experiment. SD—standard deviation.

It is worth noting that the greatest increase in the stability of the pEGCG is present in the prepared nanoformulation. Although the pEGCG concentration on the 28th day was as low as 10% of the initial concentration in both refrigerator and room temperature, free pEGCG is fully degraded in the culture medium at 37 °C over 120 min [50]. pEGCG

decomposes rapidly over the first 7 days of storage, but the decrease is much slower over the remaining 21 days, with the concentration falling from 20 to 10%.

3.3. Biological Activity

The potential of phytochemicals, which might modulate numerous signaling pathways involved in cancer development and progression has been presented in several preclinical and clinical studies [51–53]. To date, a plethora of dietary phytochemicals, such as curcumin [54], epigallocatechin-3-*O*-gallate [55], resveratrol [56], lycopene [57], sulforaphane [58], and others, have demonstrated anticancer effects, including against prostate and bladder cancers [59,60]. Although our knowledge about cancer biology is rapidly increasing, and significant progress in cancer research has been made during recent years, drug resistance development remains one of the most critical challenges in cancer treatment [61,62]. Because of the prevailing situation drugs are often administered in combinations to overcome the aforementioned problem and increase treatment efficacy. However, there are no simple and clear solutions as to which compounds should be combined and what is more how they should be administered to maximize their effectiveness. Somers-Edgar et al. showed that a combination of EGCG and curcumin used at a lower dose might lead to synergistic anticancer activity towards triple-negative breast cancer cells [63]. Also, Eom et al. found that co-treatment of EGCG and curcumin improved anticancer effects in prostate cancer PC-3 cell line [36]. However, the literature data shows that applying these two compounds might also have an antagonistic effect in that almost all phytochemicals demonstrate low bioavailability, which may further decrease their effectiveness in clinics. Thus, tremendous efforts have been made to improve their stability, release, and membrane permeation, and protection from extensive metabolic processes. In the context of EGCG, these can be done by designing nanostructure-based drug delivery systems and specific molecular modifications [64,65]. Peracetylation is a well-known modification to protect EGCG from oxidative degradation and rapid biotransformation [65]. The advantage of pEGCG was found in both in vitro and in vivo models [66–68]. Lee and coworkers found that pEGCG was more effective in suppressing the growth of androgen-independent prostate cancer in nude mice than the EGCG [69]. Other researchers have described how pEGCG might serve as a novel angiogenesis inhibitor via decreasing VEGFA secretion by endometrial cancer cells through inhibiting PI3K/AKT/mTOR/HIF1α signaling pathway [70]. Numerous basic research studies support the hypothesis that a nano-scale delivery system might improve EGCG absorption. To date, several carrier systems, including lipid-based, polymer-based, carbohydrate-based, protein-based, and metal-based nanoparticles, have been used to promote EGCG stability and absorption [71]. However, there is limited knowledge about the encapsulation of pEGCG. Thus, in the presented study, we used pEGCG instead of the commonly used EGCG [70]. Curcumin is a well-known compound that possesses pleiotropic activity, including anticancer activity. However, curcumin has not yet been approved as a therapeutic agent due to its low solubility, bioavailability, and rapid metabolism [72,73]. Like EGCG, several possibilities for overcoming drawbacks related to the insufficient absorption of curcumin have been proposed, including its structural modification and application with a proper delivery system. It was evidenced that encapsulation of curcumin in liposomes might improve its efficacy [74]. As Huang and co-workers nicely presented, curcumin can locate in the hydrophobic core, therefore rigidifying the entire lipid bilayers and, in this way, enhancing the stability of both liposomes and encapsulated compound [49]. To date, different liposomal formulations have been used to deliver curcumin. It should be highlighted the POPC-liposomes containing both curcumin and pEGCG as active compounds were presented in the herein study for the first time.

Firstly, three liposomal formulations were tested to select the non-toxic concentration range. These experiments were performed using the human androgen-dependent prostate LNCaP cells. Following the study, DOTAP:POPC-based liposomes decreased the cell viability, regardless of the ratio of POPC to DOTAP (Figure 6). Thus, only the POPC-based

formulation was used for further studies. Moreover, this formulation was also tested using a non-cancerous lung fibroblast MRC-5 cell line. The POPC at a concentration of 10% decreased MRC-5 viability to 96 and 89.71% after incubation lasting 24 and 48 h, respectively. Based on these data, the POPC concentration should not exceed 5%.

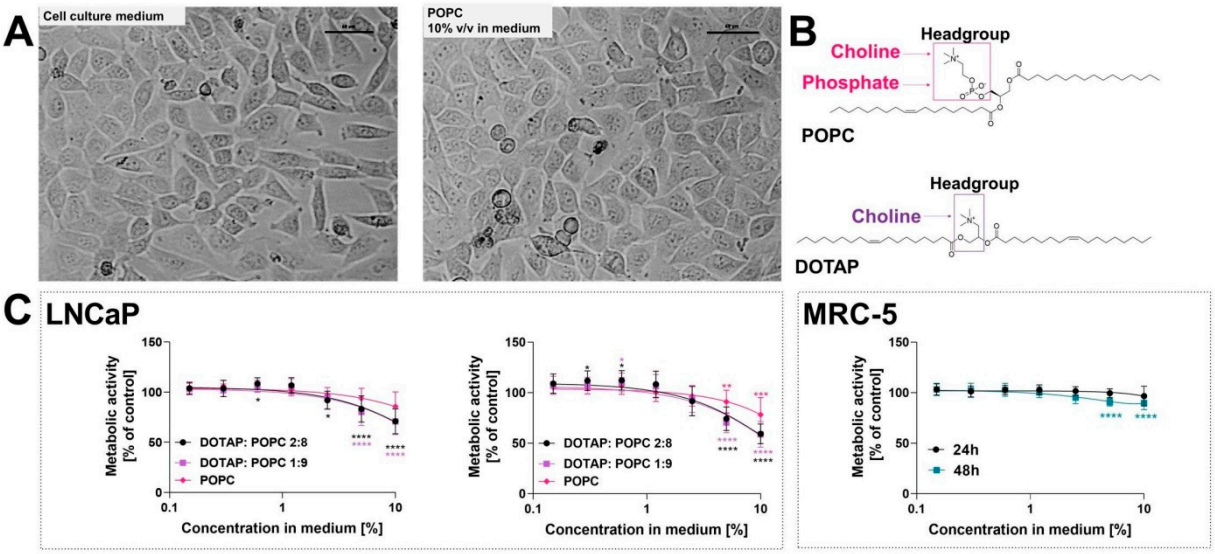

Figure 6. The cytotoxicity of the tested liposomal formulation. Panel (**A**) presents the cell morphology after incubation with POPC liposomes and cell culture medium after 48 h incubation time (representative images). The images were taken with a DS-SMc digital camera attached to a Nikon Eclipse TS100 microscope. Scale bar corresponds to 50 µm; panel (**B**) presents the chemical structure of 1-palmitoyl-2-oleoyl-sn-glycero-3-phosphocholine (POPC) and 1,2-dioleoyl-3-trimethylammonium-propane (DOTAP); panel (**C**) presents the effect of the tested empty liposomal formulations on cell viability. The DOTAP:POPC 1:9, DOTAP:POPC 2:8, and POPC liposomes were added to a cell culture medium at a concentration of 0.15–10% v/v for 24 and 48 h. The cell viability was measured by MTT assay. A cell culture medium was used as a control. The selected formulation was tested on a non-cancerous human lung fibroblast MRC-5 cell line. Data are expressed as the mean ± SD from five experiments (POPC, LNCaP), four experiments (DOTAP:POPC, LNCaP), and three experiments (for MRC-5). Statistical significance between groups was assessed by Dunnett's Multiple Comparison Test (* $p < 0.05$; ** $p < 0.01$, *** $p < 0.001$; **** $p < 0.0001$).

To determine the cytotoxic activity of tested compounds in their free form, the 5637, LNCaP, and MRC-5 cells were treated with CUR and pEGCG dissolved in DMSO (Table 5). The most sensitive to curcumin was the 5637 cell line with IC_{50} values of 17.95 ± 6.68 µm and 11.25 ± 2.47 µm after incubation lasting 24 h, and 48 h, respectively. Our findings align with data reported by Konstantinov and co-workers, where the curcumin IC_{50} was 14.28 µm for 5637 cells [75]. Also, Hauser et al. showed the cytotoxic activity of curcumin towards a panel of urothelial bladder cancer cell lines after treatment lasting 48 h (IC_{50} value of 10.5 ± 1 µm for 5637 cells) [76]. In our work, the IC_{50} values for LNCaP cells were 30.61 ± 6.95 µm and 19.66 ± 3.78 µm after 24 and 48 h of curcumin treatment, respectively. Choi and co-workers also observed similar activity against LNCaP cells. The antiproliferative effect of curcumin was measured using the MTS assay, and the IC_{50} of curcumin after 24 and 48 h treatment was 25.0 and 18.4 µm, respectively [77]. Also, Eslami et al. showed that the IC_{50} for curcumin using the MTT assay was 25.01 and 18.66 µm for 24 and 48 h, respectively [78]. In our study, the highest IC_{50} was calculated for normal human lung fibroblast MRC-5 (38.73 ± 3.39 µm and 25.81 ± 1.61 µm) for 24 and 48 h, respectively). Dhima et al. focused on curcumin's ability to sensitize leiomyosarcoma (LMS) cells to cisplatin and also determined the cytotoxicity against MRC-5 cells with the IC_{50} value of 47.2 ± 5.1 µm after 48 h of treatment [79]. On the other hand, Muthoosamy et al.

did not observe the cytotoxic effect of curcumin in MRC-5 cells (the IC_{50} > 200 μg/mL) [80]. The literature data shows that cancer cells are more sensitive to curcumin than normal cells. However, curcumin may also affect normal cells depending on the cell types. It was found that curcumin at a concentration of 10 μm might inhibit cellular proliferation through G2/M cell cycle phase arrest in human dermal fibroblasts (HDFs) [81].

Table 5. The IC_{50} values of curcumin, pEGCG, and their combinations dissolved in DMSO. Data are expressed as the mean ± SD from at least three independent experiments; only pEGCG for 5637 cell line presents mean from two independent experiments.

	IC_{50} [μM]			
Cell Line	**Curcumin**		**pEGCG**	
	24 h	**48 h**	**24 h**	**48 h**
5637	17.95 ± 6.68	11.25 ± 2.47	84.08 ± 1.09	76.73 ± 0.24
LNCaP	30.61 ± 6.95	19.66 ± 3.78	62.45 ± 12.10	60.98 ± 9.25
MRC-5	38.73 ± 3.39	25.81 ± 1.61	73.82 ± 6.23	65.55 ± 5.92

The pEGCG exerted less cytotoxic activity against all tested cells than curcumin. Interestingly, the pECGC expressed higher activity against LNCaP cells, while the 5637 cells were less sensitive to pEGCG. Shenouda et al. reported that the IC_{50} of EGCG on LNCaP cells was 100 μm [82], while Luo et al. showed that EGCG inhibited the growth of 5637 cells with an IC_{50} value of 69.5 μm [83]. However, there is no research indicating the cytotoxicity of peracetylated EGCG against LNCaP and 5637 cell lines.

The IC_{50} values of the liposomal formulation of tested compounds and their combination are presented in Table 6, and the dose-response curves are presented in Figure 7. The IC_{50} values for curcumin and curcumin encapsulated in POPC liposomes are comparable for 5637 cells. For the free form, the IC_{50} values were 17.95 ± 6.68 μm and 11.25 ± 2.47 μm for 24 and 48 h, respectively; while for the liposomal formulation, IC_{50} reached the values of 17.12 ± 4.09 μm and 12.27 ± 2.91 μm for 24 and 48 h incubation time, respectively. LNCaP cells also responded similarly to curcumin treatment. At the doses used for this experiment, pEGCG did not significantly affect the viability of either of the cell lines. These results clearly show that it is CUR, which is responsible for the cytotoxic effects within this combination of ingredients. For 5637 and LNCaP cells, the curcumin showed comparable suppression of cell viability for liposomal formulation and the free form in DMSO. Interestingly, the cytotoxic activity of curcumin against normal fibroblast was lower in liposomal formulation compared to curcumin dissolved in DMSO. To date, the curcumin-loaded POPC-based liposomes were studied towards the protective activity against dental pulp stem cells (hDPSCs) [84]. The authors found that curcumin in POPC at the concentration of 20 μm did not affect cell viability. Moreover, liposomal formulation increased hDPSCs' proliferation and inhibited inflammatory cytokines secretion by regulating NFkB/ERK and pERK signaling cascades [84]. The POPC-based liposomes were also used to design the theranostic system that combined curcumin and bis(2,4,6-trichlorphenyl)oxalate (TCPO) to detect oxidative stress in cancer cells [85]. Curcumin acts as a fluorochrome in this system, while TCPO is an inducer for peroxyoxalate chemiluminescence (PO-CL) reaction [85]. In the proposed mechanism for PO-CL reaction, an oxalic acid derivative (TCPO) reacts with hydrogen peroxide to generate intermediate 1,2-dioxetanedione, which does not emit light but transfers its energy to a fluorescent molecule (curcumin) emitting light after relaxation to the ground state [85]. However, both curcumin and TCPO are hydrophobic and degrade in an aqueous environment; the POPC-based liposomal formulation was used to deliver this cargo into cells. Moreover, the authors reported that the interaction of curcumin with the POPC liposomes might stabilize the structure and minimize curcumin degradation [85]. However, there is no evidence of cytotoxicity of curcumin–POPC liposomes against bladder and prostate cancer cells.

Table 6. The IC_{50} values of curcumin, pEGCG, and their combination in liposomes. Data are expressed as the mean ± SD from three independent experiments.

Cell Line	Curcumin		pEGCG		Curcumin+pEGCG	
	24 h	48 h	24 h	48 h	24 h	48 h
5637	17.12 ± 4.09	12.27 ± 2.91	>40	>40	19.50 ± 3.23	15.33 ± 2.03
LNCaP	38.96 ± 2.90	22.06 ± 3.14	>40	>40	>40	>40
MRC-5	>40	>40	>40	>40	>40	>40

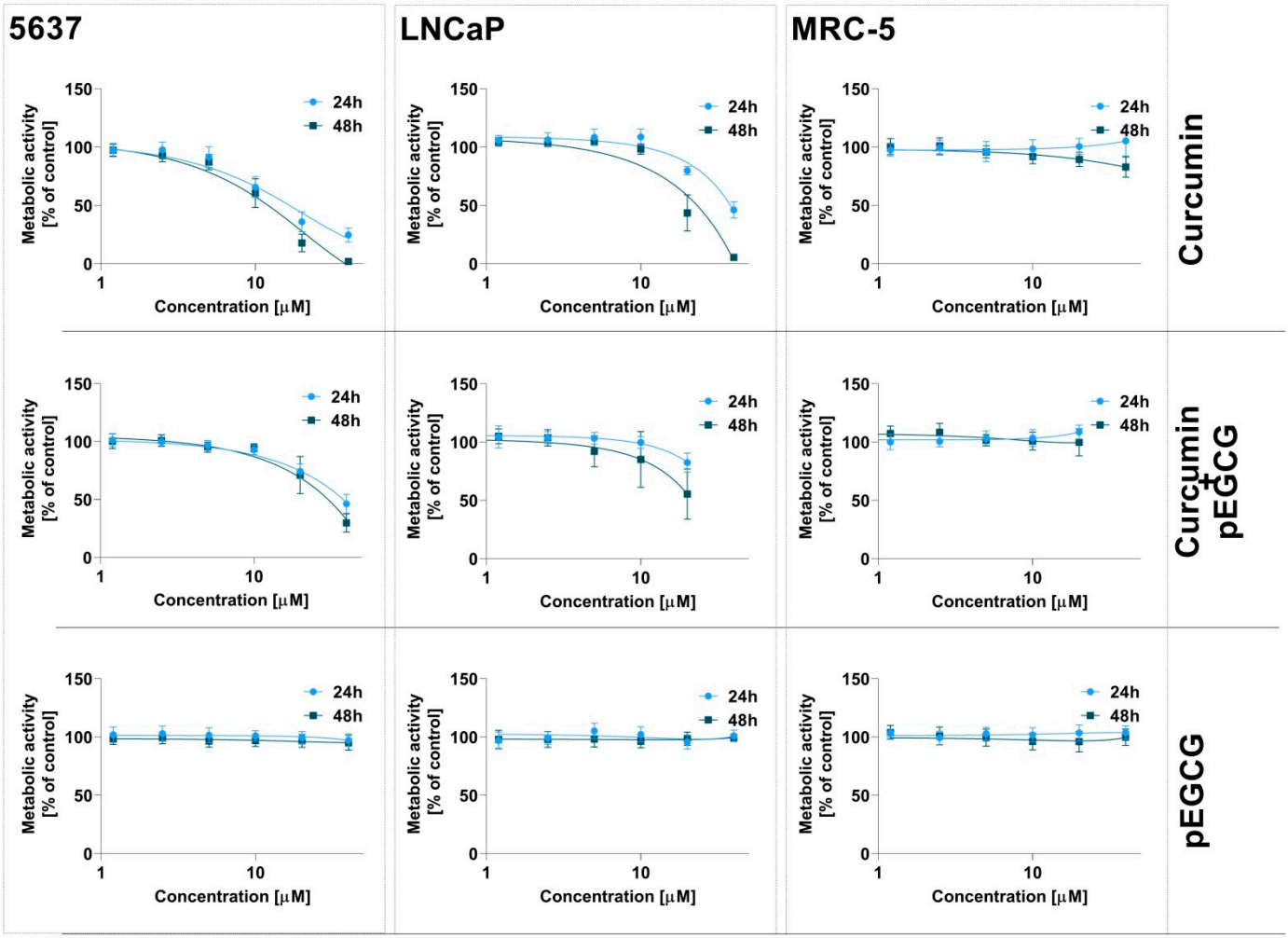

Figure 7. The cytotoxic activity of liposomal formulation containing curcumin, pEGCG, and their combination against 5637, LNCaP, and MRC-5 cells. Data are expressed as the mean ± SD from three independent experiments.

The presented results confirm the possibility of using POPC liposomes instead of DMSO solutions in vitro. These results also suggest that the tested formulation might be considered for in vivo experiments. However, further in vivo studies should be performed to verify the lack of toxicity of the empty liposomal formulation. Scientific research demonstrates the negative impact of DMSO on biological assays. Verheijen et al. demonstrated the ability of DMSO to induce changes in cellular processes, which may significantly influence the formulated conclusions, e.g., regarding drug toxicity [86]. Galvao and co-workers reported that the final concentration of DMSO, even used at a low concentration—0.1% (*v*/*v*)—is toxic in vivo and leads to significant retinal apoptosis [87]. Thus, other formulations, e.g., liposomes, are more favorable than DMSO as a drug solvent. The authors also

recommended that the percentage of DMSO used to dissolve drugs be kept to a minimum (1% *v/v* solutions for injections) and highlighted the need to include an additional untreated control group to verify the potential solvent toxic effects [87]. Therefore, the use of liposomes fits perfectly with the 3Rs rule (reducement, refinement, replacement) by reducing the number of animals needed for study and avoiding potential side effects. To obtain the desirable results it is important to consider the injection of pEGCG or curcumin, which would have to be used at relatively high concentrations.

Phytochemicals might interact with each other, promoting the effectiveness of the compounds via synergistic or additive effects. However, different bioactive compounds might also block or reduce their activity (antagonistic effect) [88]. The observed combinatorial effect of CUR and pEGCG was slightly antagonistic rather than synergistic (Figure 8). The combination of CUR with pEGCG at the tested concentration range led to the decreased activity of curcumin in 5637 and LNCaP cells. As was noted by Ghosh et al., administration of curcumin simultaneously with EGCG is associated with antagonistic activity towards primary chronic lymphocytic leukemia (CLL) B cells [89]. In contrast, sequential administration of these compounds increases cell death via apoptosis pathway, compared to the treatment with the individual agent alone [89]. Thus, it appears that pEGCG might exert a similar effect as EGCG when it comes to decreasing CUR activity. Admittedly, our study is not free from several limitations, including only one tested molar ratio of CUR and pEGCG and only simultaneous administration of both compounds. It is well-known that after administration, firstly, each nanoparticle will be exposed to a complex biological fluid, such as serum, that is rich in various proteins. Thus, the liposome surface is coated mainly by proteins to form a biomolecular corona (BMC) in the living system [90], and this phenomenon might affect liposome stability and size [91–93]. Thus, considering this critical aspect of the liposomal-based drug delivery, further studies focusing on the behavior of tested formulations in cell culture medium must be performed to better predict their potential use in in vivo models. However, our findings present important knowledge about the potential interaction of CUR and pEGCG used at relatively low concentrations. Furthermore, our results showed that curcumin encapsulated in POPC exerted a lower cytotoxic effect against non-cancerous cells.

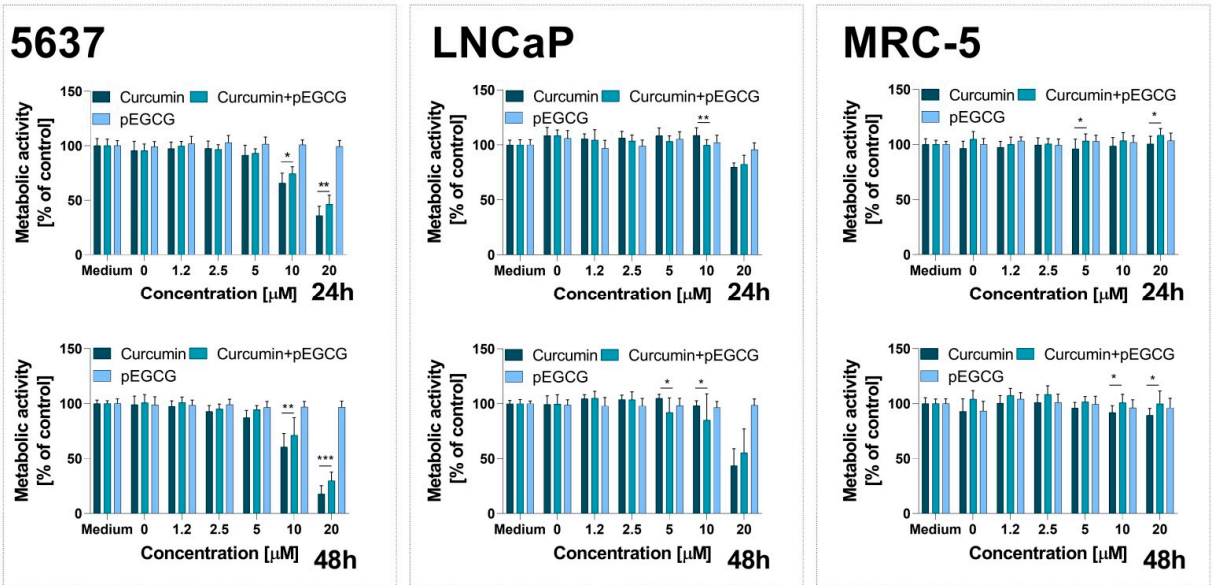

Figure 8. The comparison of curcumin, pEGCG, and combination of both compounds in liposomes against 5637, LNCaP, and MRC-5 cells. Data are expressed as the mean ± SD from three experiments. Statistical significance between groups was assessed by Tukey's Comparison Test (* $p < 0.05$; ** $p < 0.01$, *** $p < 0.001$).

4. Conclusions

The presented studies proved the possibility of encapsulating two different polyphenols (CUR and pEGCG) in liposomes (POPC) at two temperature levels, i.e., at room temperature (20 °C) and in a refrigerator (4–8 °C). Such a combination allowed to increase the stability of CUR in CUR + pEGCG/POPC formulation to a more significant extent than in CUR/POPC formulation at refrigerator temperature (51 and 41% of the initial concentration, respectively). In addition, the closed environment provided by liposomes, increases stability of pEGCGs and does not lead to complete degradation, resulting in 10–11% of the initial concentration of pEGCG at the end of the studied period. Notably, the maximum concentration of CUR in POPC liposomes has been designated at 1 666 µm, limiting the possible toxic effects of lipids on cells. What is more, the cytotoxic effect of liposome-encapsulated CUR on bladder cancer cells (5637 cell line) was demonstrated for the first time with IC_{50} calculated at 19.50 ± 3.23 µm and 15.33 ± 2.03 µm after 24 and 48 h, respectively. Moreover, the presented results confirm the possibility of using POPC liposomes instead of DMSO solutions in the in vitro tests, which has great significance when translating the in vitro to in vivo studies. The presented research provides new possibilities for applying selected polyphenols to urogenital neoplasms, including the use of the potential provided by the encapsulation in liposomes to targeted therapy. This methodology could be a promising tool to increase the concentration of CUR and pEGCG through their precise delivery into cancer cells.

Author Contributions: Conceptualization, L.P. and D.T.M.; Data curation, J.P., T.G. and A.J.; Formal analysis, L.P., M.K. and D.T.M.; Funding acquisition, T.G. and A.J.; Investigation, L.P., M.K. and S.T.; Methodology, L.P., M.K., D.T.M. and J.P.; Resources, T.G.; Software, L.P., S.T. and D.T.M.; Supervision, T.G., M.M. and A.J.; Validation, L.P., M.K., S.T., D.T.M. and A.J.; Visualization, L.P. and D.T.M.; Writing—original draft, L.P., M.K., S.T. and D.T.M.; Writing—review and editing, T.G., M.M. and A.J. All authors have read and agreed to the published version of the manuscript.

Funding: This research was funded by National Science Centre, Poland, grant number 2019/35/B/NZ7/01165.

Institutional Review Board Statement: Not applicable.

Informed Consent Statement: Not applicable.

Data Availability Statement: All the data obtained in this study is presented in the article.

Acknowledgments: Authors acknowledge the generous gift of EGCG from Jerzy Jankun. Figure 2 was created with BioRender.com (under the appropriate license), and using Servier Medical Art (Servier, www.servier.com, accessed on 10 January 2022, licensed under a Creative Commons Attribution 3.0 Unported Licence).

Conflicts of Interest: The authors declare no conflict of interest. The funders had no role in the design of the study; in the collection, analyses, or interpretation of data; in the writing of the manuscript, or in the decision to publish the results.

References

1. Hass, R.; Jennek, S.; Yang, Y.; Friedrich, K. C-Met Expression and Activity in Urogenital Cancers—Novel Aspects of Signal Transduction and Medical Implications. *Cell Commun. Signal.* **2017**, *15*, 10. [CrossRef]
2. Saginala, K.; Barsouk, A.; Aluru, J.S.; Rawla, P.; Padala, S.A.; Barsouk, A. Epidemiology of Bladder Cancer. *Med. Sci.* **2020**, *8*, 15. [CrossRef] [PubMed]
3. Zaghloul, M.S.; Zaghloul, T.M.; Bishr, M.K.; Baumann, B.C. Urinary Schistosomiasis and the Associated Bladder Cancer: Update. *J. Egypt. Natl. Cancer Inst.* **2020**, *32*, 44. [CrossRef] [PubMed]
4. Lenis, A.T.; Lec, P.M.; Chamie, K.; Mshs, M.D. Bladder Cancer: A Review. *JAMA* **2020**, *324*, 1980–1991. [CrossRef] [PubMed]
5. Magers, M.J.; Lopez-Beltran, A.; Montironi, R.; Williamson, S.R.; Kaimakliotis, H.Z.; Cheng, L. Staging of Bladder Cancer. *Histopathology* **2019**, *74*, 112–134. [CrossRef] [PubMed]
6. Piwowarczyk, L.; Stawny, M.; Mlynarczyk, D.T.; Muszalska-Kolos, I.; Goslinski, T.; Jelińska, A. Role of Curcumin and (−)-Epigallocatechin-3-O-Gallate in Bladder Cancer Treatment: A Review. *Cancers* **2020**, *12*, 1801. [CrossRef]
7. De George, K.C.; Holt, H.R.; Hodges, S.C. Bladder Cancer: Diagnosis and Treatment. *Am. Fam. Physician* **2017**, *96*, 507–514.

8. Babjuk, M.; Böhle, A.; Burger, M.; Capoun, O.; Cohen, D.; Compérat, E.M.; Hernández, V.; Kaasinen, E.; Palou, J.; Rouprêt, M.; et al. EAU Guidelines on Non-Muscle-Invasive Urothelial Carcinoma of the Bladder: Update 2016. *Eur. Urol.* **2017**, *71*, 447–461. [CrossRef]
9. Teo, M.Y.; Rathkopf, D.E.; Kantoff, P. Treatment of Advanced Prostate Cancer. *Annu. Rev. Med.* **2019**, *70*, 479–499. [CrossRef]
10. Cory, H.; Passarelli, S.; Szeto, J.; Tamez, M.; Mattei, J. The Role of Polyphenols in Human Health and Food Systems: A Mini-Review. *Front. Nutr.* **2018**, *5*, 87. [CrossRef]
11. Min, K.; Kwon, T.K. Anticancer Effects and Molecular Mechanisms of Epigallocatechin-3-Gallate. *Integr. Med. Res.* **2014**, *3*, 16–24. [CrossRef] [PubMed]
12. Krupkova, O.; Ferguson, S.J.; Wuertz-Kozak, K. Stability of (−)-Epigallocatechin Gallate and Its Activity in Liquid Formulations and Delivery Systems. *J. Nutr. Biochem.* **2016**, *37*, 1–12. [CrossRef]
13. Pari, L.; Tewas, D.; Eckel, J. Role of Curcumin in Health and Disease. *Arch. Physiol. Biochem.* **2008**, *114*, 127–149. [CrossRef]
14. Rahmani, A.H.; Alsahli, M.A.; Aly, S.M.; Khan, M.A.; Aldebasi, Y.H. Role of Curcumin in Disease Prevention and Treatment. *Adv. Biomed. Res.* **2018**, *7*, 38. [CrossRef]
15. Sharifi-Rad, J.; Rayess, Y.E.; Rizk, A.A.; Sadaka, C.; Zgheib, R.; Zam, W.; Sestito, S.; Rapposelli, S.; Neffe-Skocińska, K.; Zielińska, D.; et al. Turmeric and Its Major Compound Curcumin on Health: Bioactive Effects and Safety Profiles for Food, Pharmaceutical, Biotechnological and Medicinal Applications. *Front. Pharmacol.* **2020**, *11*, 01021. [CrossRef]
16. A Novel Curcumin Derivative Which Inhibits P-Glycoprotein, Arrests Cell Cycle and Induces Apoptosis in Multidrug Resistance Cells—ScienceDirect. Available online: https://www.sciencedirect.com/science/article/abs/pii/S0968089616311890 (accessed on 30 December 2021).
17. Maleki Dizaj, S.; Alipour, M.; Dalir Abdolahinia, E.; Ahmadian, E.; Eftekhari, A.; Forouhandeh, H.; Rahbar Saadat, Y.; Sharifi, S.; Zununi Vahed, S. Curcumin Nanoformulations: Beneficial Nanomedicine against Cancer. *Phytother. Res.* **2022**, *36*, 1156–1181. [CrossRef] [PubMed]
18. Karthikeyan, A.; Senthil, N.; Min, T. Nanocurcumin: A Promising Candidate for Therapeutic Applications. *Front. Pharmacol.* **2020**, *11*, 487. [CrossRef] [PubMed]
19. Liu, G.; Hou, S.; Tong, P.; Li, J. Liposomes: Preparation, Characteristics, and Application Strategies in Analytical Chemistry. *Crit. Rev. Anal. Chem.* **2022**, *52*, 392–412. [CrossRef]
20. Patil, Y.P.; Jadhav, S. Novel Methods for Liposome Preparation. *Chem. Phys. Lipids* **2014**, *177*, 8–18. [CrossRef]
21. Li, M.; Du, C.; Guo, N.; Teng, Y.; Meng, X.; Sun, H.; Li, S.; Yu, P.; Galons, H. Composition Design and Medical Application of Liposomes. *Eur. J. Med. Chem.* **2019**, *164*, 640–653. [CrossRef]
22. Liu, P.; Chen, G.; Zhang, J. A Review of Liposomes as a Drug Delivery System: Current Status of Approved Products, Regulatory Environments, and Future Perspectives. *Molecules* **2022**, *27*, 1372. [CrossRef] [PubMed]
23. Kohri, T.; Nanjo, F.; Suzuki, M.; Seto, R.; Matsumoto, N.; Yamakawa, M.; Hojo, H.; Hara, Y.; Desai, D.; Amin, S.; et al. Synthesis of (−)-[4-^{3}H]Epigallocatechin Gallate and Its Metabolic Fate in Rats after Intravenous Administration. *J. Agric. Food Chem.* **2001**, *49*, 1042–1048. [CrossRef]
24. Piskorz, J.; Mlynarczyk, D.T.; Szczolko, W.; Konopka, K.; Düzgüneş, N.; Mielcarek, J. Liposomal Formulations of Magnesium Sulfanyl Tribenzoporphyrazines for the Photodynamic Therapy of Cancer. *J. Inorg. Biochem.* **2018**, *184*, 34–41. [CrossRef] [PubMed]
25. Hudiyanti, D.; Khafiz, M.F.A.; Anam, K.; Siahaan, P.; Suyati, L. Assessing Encapsulation of Curcumin in Cocoliposome: In Vitro Study. *Open Chem.* **2021**, *19*, 358–366. [CrossRef]
26. Zhang, H. Thin-Film Hydration Followed by Extrusion Method for Liposome Preparation. *Methods Mol. Biol.* **2017**, *1522*, 17–22. [CrossRef] [PubMed]
27. Shimoda, A.; Tahara, Y.; Sawada, S.; Sasaki, Y.; Akiyoshi, K. Glycan Profiling Analysis Using Evanescent-Field Fluorescence-Assisted Lectin Array: Importance of Sugar Recognition for Cellular Uptake of Exosomes from Mesenchymal Stem Cells. *Biochem. Biophys. Res. Commun.* **2017**, *491*, 701–707. [CrossRef] [PubMed]
28. Filipe, V.; Hawe, A.; Jiskoot, W. Critical Evaluation of Nanoparticle Tracking Analysis (NTA) by NanoSight for the Measurement of Nanoparticles and Protein Aggregates. *Pharm. Res.* **2010**, *27*, 796–810. [CrossRef]
29. Sato, Y.T.; Umezaki, K.; Sawada, S.; Mukai, S.; Sasaki, Y.; Harada, N.; Shiku, H.; Akiyoshi, K. Engineering Hybrid Exosomes by Membrane Fusion with Liposomes. *Sci. Rep.* **2016**, *6*, 21933. [CrossRef]
30. van Meerloo, J.; Kaspers, G.J.L.; Cloos, J. Cell Sensitivity Assays: The MTT Assay. In *Cancer Cell Culture: Methods and Protocols*; Cree, I.A., Ed.; Methods in Molecular Biology; Humana Press: Totowa, NJ, USA, 2011; pp. 237–245. ISBN 978-1-61779-080-5.
31. Mosmann, T. Rapid Colorimetric Assay for Cellular Growth and Survival: Application to Proliferation and Cytotoxicity Assays. *J. Immunol. Methods* **1983**, *65*, 55–63. [CrossRef]
32. Kucinska, M.; Piotrowska-Kempisty, H.; Lisiak, N.; Kaczmarek, M.; Dams-Kozlowska, H.; Granig, W.H.; Höferl, M.; Jäger, W.; Zehl, M.; Murias, M.; et al. Selective Anticancer Activity of the Novel Thiobenzanilide 63T against Human Lung Adenocarcinoma Cells. *Toxicol. Vitr.* **2016**, *37*, 148–161. [CrossRef]
33. Yan, X.; Zhang, X.; McClements, D.J.; Zou, L.; Liu, X.; Liu, F. Co-Encapsulation of Epigallocatechin Gallate (EGCG) and Curcumin by Two Proteins-Based Nanoparticles: Role of EGCG. *J. Agric. Food Chem.* **2019**, *67*, 13228–13236. [CrossRef] [PubMed]
34. Chung, S.S.; Vadgama, J.V. Curcumin and Epigallocatechin Gallate Inhibit the Cancer Stem Cell Phenotype via Down-Regulation of STAT3–NFκB Signaling. *Anticancer Res.* **2015**, *35*, 39–46. [PubMed]

35. Jin, G.; Yang, Y.; Liu, K.; Zhao, J.; Chen, X.; Liu, H.; Bai, R.; Li, X.; Jiang, Y.; Zhang, X.; et al. Combination Curcumin and (−)-Epigallocatechin-3-Gallate Inhibits Colorectal Carcinoma Microenvironment-Induced Angiogenesis by JAK/STAT3/IL-8 Pathway. *Oncogenesis* **2017**, *6*, e384. [CrossRef] [PubMed]
36. Eom, D.-W.; Lee, J.H.; Kim, Y.-J.; Hwang, G.S.; Kim, S.-N.; Kwak, J.H.; Cheon, G.J.; Kim, K.H.; Jang, H.-J.; Ham, J.; et al. Synergistic Effect of Curcumin on Epigallocatechin Gallate-Induced Anticancer Action in PC3 Prostate Cancer Cells. *BMB Rep.* **2015**, *48*, 461–466. [CrossRef]
37. Inglut, C.T.; Sorrin, A.J.; Kuruppu, T.; Vig, S.; Cicalo, J.; Ahmad, H.; Huang, H.-C. Immunological and Toxicological Considerations for the Design of Liposomes. *Nanomaterials* **2020**, *10*, 190. [CrossRef]
38. Arab-Tehrany, E.; Elkhoury, K.; Francius, G.; Jierry, L.; Mano, J.F.; Kahn, C.; Linder, M. Curcumin Loaded Nanoliposomes Localization by Nanoscale Characterization. *Int. J. Mol. Sci.* **2020**, *21*, 7276. [CrossRef]
39. Wu, Y.; Mou, B.; Song, S.; Tan, C.-P.; Lai, O.-M.; Shen, C.; Cheong, L.-Z. Curcumin-Loaded Liposomes Prepared from Bovine Milk and Krill Phospholipids: Effects of Chemical Composition on Storage Stability, in-Vitro Digestibility and Anti-Hyperglycemic Properties. *Food Res. Int.* **2020**, *136*, 109301. [CrossRef]
40. Farokhzad, O.C.; Langer, R. Impact of Nanotechnology on Drug Delivery. *ACS Nano* **2009**, *3*, 16–20. [CrossRef]
41. Lombardo, D.; Calandra, P.; Barreca, D.; Magazù, S.; Kiselev, M.A. Soft Interaction in Liposome Nanocarriers for Therapeutic Drug Delivery. *Nanomaterials* **2016**, *6*, 125. [CrossRef]
42. de Morais Ribeiro, L.N.; Couto, V.M.; Fraceto, L.F.; de Paula, E. Use of Nanoparticle Concentration as a Tool to Understand the Structural Properties of Colloids. *Sci. Rep.* **2018**, *8*, 982. [CrossRef]
43. Clayton, K.N.; Salameh, J.W.; Wereley, S.T.; Kinzer-Ursem, T.L. Physical Characterization of Nanoparticle Size and Surface Modification Using Particle Scattering Diffusometry. *Biomicrofluidics* **2016**, *10*, 054107. [CrossRef] [PubMed]
44. Smith, M.C.; Crist, R.M.; Clogston, J.D.; McNeil, S.E. Zeta Potential: A Case Study of Cationic, Anionic, and Neutral Liposomes. *Anal. Bioanal. Chem.* **2017**, *409*, 5779–5787. [CrossRef]
45. Varga, Z.; Fehér, B.; Kitka, D.; Wacha, A.; Bóta, A.; Berényi, S.; Pipich, V.; Fraikin, J.-L. Size Measurement of Extracellular Vesicles and Synthetic Liposomes: The Impact of the Hydration Shell and the Protein Corona. *Colloids Surf. B Biointerfaces* **2020**, *192*, 111053. [CrossRef] [PubMed]
46. Tai, K.; Rappolt, M.; Mao, L.; Gao, Y.; Yuan, F. Stability and Release Performance of Curcumin-Loaded Liposomes with Varying Content of Hydrogenated Phospholipids. *Food Chem.* **2020**, *326*, 126973. [CrossRef] [PubMed]
47. Danaei, M.; Dehghankhold, M.; Ataei, S.; Hasanzadeh Davarani, F.; Javanmard, R.; Dokhani, A.; Khorasani, S.; Mozafari, M.R. Impact of Particle Size and Polydispersity Index on the Clinical Applications of Lipidic Nanocarrier Systems. *Pharmaceutics* **2018**, *10*, 57. [CrossRef] [PubMed]
48. Badran, M.; Shalaby, K.; Al-Omrani, A. Influence of the Flexible Liposomes on the Skin Deposition of a Hydrophilic Model Drug, Carboxyfluorescein: Dependency on Their Composition. *Sci. World J.* **2012**, *2012*, e134876. [CrossRef]
49. Huang, M.; Liang, C.; Tan, C.; Huang, S.; Ying, R.; Wang, Y.; Wang, Z.; Zhang, Y. Liposome Co-Encapsulation as a Strategy for the Delivery of Curcumin and Resveratrol. *Food Funct.* **2019**, *10*, 6447–6458. [CrossRef]
50. Lam, W.H.; Kazi, A.; Kuhn, D.J.; Chow, L.M.C.; Chan, A.S.C.; Ping Dou, Q.; Chan, T.H. A Potential Prodrug for a Green Tea Polyphenol Proteasome Inhibitor: Evaluation of the Peracetate Ester of (−)-Epigallocatechin Gallate [(−)-EGCG]. *Bioorganic Med. Chem.* **2004**, *12*, 5587–5593. [CrossRef]
51. Lodi, A.; Saha, A.; Lu, X.; Wang, B.; Sentandreu, E.; Collins, M.; Kolonin, M.G.; DiGiovanni, J.; Tiziani, S. Combinatorial Treatment with Natural Compounds in Prostate Cancer Inhibits Prostate Tumor Growth and Leads to Key Modulations of Cancer Cell Metabolism. *NPJ Precis. Oncol.* **2017**, *1*, 18. [CrossRef]
52. Akhtar, M.F.; Saleem, A.; Rasul, A.; Faran Ashraf Baig, M.M.; Bin-Jumah, M.; Abdel Daim, M.M. Anticancer Natural Medicines: An Overview of Cell Signaling and Other Targets of Anticancer Phytochemicals. *Eur. J. Pharmacol.* **2020**, *888*, 173488. [CrossRef]
53. Chirumbolo, S.; Bjørklund, G.; Lysiuk, R.; Vella, A.; Lenchyk, L.; Upyr, T. Targeting Cancer with Phytochemicals via Their Fine Tuning of the Cell Survival Signaling Pathways. *Int. J. Mol. Sci.* **2018**, *19*, 3568. [CrossRef]
54. Rutz, J.; Janicova, A.; Woidacki, K.; Chun, F.K.-H.; Blaheta, R.A.; Relja, B. Curcumin—A Viable Agent for Better Bladder Cancer Treatment. *Int. J. Mol. Sci.* **2020**, *21*, 3761. [CrossRef]
55. Miyata, Y.; Shida, Y.; Hakariya, T.; Sakai, H. Anti-Cancer Effects of Green Tea Polyphenols Against Prostate Cancer. *Molecules* **2019**, *24*, 193. [CrossRef]
56. Zaffaroni, N.; Beretta, G.L. Resveratrol and Prostate Cancer: The Power of Phytochemicals. *Curr. Med. Chem.* **2021**, *28*, 4845–4862. [CrossRef]
57. Mirahmadi, M.; Azimi-Hashemi, S.; Saburi, E.; Kamali, H.; Pishbin, M.; Hadizadeh, F. Potential Inhibitory Effect of Lycopene on Prostate Cancer. *Biomed. Pharmacother.* **2020**, *129*, 110459. [CrossRef]
58. Leone, A.; Diorio, G.; Sexton, W.; Schell, M.; Alexandrow, M.; Fahey, J.W.; Kumar, N.B. Sulforaphane for the Chemoprevention of Bladder Cancer: Molecular Mechanism Targeted Approach. *Oncotarget* **2017**, *8*, 35412–35424. [CrossRef]
59. Salehi, B.; Fokou, P.V.T.; Yamthe, L.R.T.; Tali, B.T.; Adetunji, C.O.; Rahavian, A.; Mudau, F.N.; Martorell, M.; Setzer, W.N.; Rodrigues, C.F.; et al. Phytochemicals in Prostate Cancer: From Bioactive Molecules to Upcoming Therapeutic Agents. *Nutrients* **2019**, *11*, 1483. [CrossRef]
60. Xia, Y.; Chen, R.; Lu, G.; Li, C.; Lian, S.; Kang, T.-W.; Jung, Y.D. Natural Phytochemicals in Bladder Cancer Prevention and Therapy. *Front. Oncol.* **2021**, *11*, 652033. [CrossRef]

61. Vasan, N.; Baselga, J.; Hyman, D.M. A View on Drug Resistance in Cancer. *Nature* **2019**, *575*, 299–309. [CrossRef]
62. Nikolaou, M.; Pavlopoulou, A.; Georgakilas, A.G.; Kyrodimos, E. The Challenge of Drug Resistance in Cancer Treatment: A Current Overview. *Clin. Exp. Metastasis* **2018**, *35*, 309–318. [CrossRef]
63. Somers-Edgar, T.J.; Scandlyn, M.J.; Stuart, E.C.; Le Nedelec, M.J.; Valentine, S.P.; Rosengren, R.J. The Combination of Epigallocatechin Gallate and Curcumin Suppresses ER Alpha-Breast Cancer Cell Growth in Vitro and in Vivo. *Int. J. Cancer* **2008**, *122*, 1966–1971. [CrossRef] [PubMed]
64. Dai, W.; Ruan, C.; Zhang, Y.; Wang, J.; Han, J.; Shao, Z.; Sun, Y.; Liang, J. Bioavailability Enhancement of EGCG by Structural Modification and Nano-Delivery: A Review. *J. Funct. Foods* **2020**, *65*, 103732. [CrossRef]
65. Cai, Z.-Y.; Li, X.-M.; Liang, J.-P.; Xiang, L.-P.; Wang, K.-R.; Shi, Y.-L.; Yang, R.; Shi, M.; Ye, J.-H.; Lu, J.-L.; et al. Bioavailability of Tea Catechins and Its Improvement. *Molecules* **2018**, *23*, 2346. [CrossRef]
66. Lambert, J.D.; Sang, S.; Hong, J.; Kwon, S.-J.; Lee, M.-J.; Ho, C.-T.; Yang, C.S. Peracetylation as a Means of Enhancing in Vitro Bioactivity and Bioavailability of Epigallocatechin-3-Gallate. *Drug Metab. Dispos.* **2006**, *34*, 2111–2116. [CrossRef] [PubMed]
67. Chiou, Y.-S.; Ma, N.J.-L.; Sang, S.; Ho, C.-T.; Wang, Y.-J.; Pan, M.-H. Peracetylated (−)-Epigallocatechin-3-Gallate (AcEGCG) Potently Suppresses Dextran Sulfate Sodium-Induced Colitis and Colon Tumorigenesis in Mice. *J. Agric. Food Chem.* **2012**, *60*, 3441–3451. [CrossRef]
68. Chao, J.; Lau, W.K.-W.; Huie, M.J.; Ho, Y.-S.; Yu, M.-S.; Lai, C.S.-W.; Wang, M.; Yuen, W.-H.; Lam, W.H.; Chan, T.H.; et al. A Pro-Drug of the Green Tea Polyphenol (−)-Epigallocatechin-3-Gallate (EGCG) Prevents Differentiated SH-SY5Y Cells from Toxicity Induced by 6-Hydroxydopamine. *Neurosci. Lett.* **2010**, *469*, 360–364. [CrossRef] [PubMed]
69. Lee, S.-C.; Chan, W.-K.; Lee, T.-W.; Lam, W.-H.; Wang, X.; Chan, T.-H.; Wong, Y.-C. Effect of a Prodrug of the Green Tea Polyphenol (-)-Epigallocatechin-3-Gallate on the Growth of Androgen-Independent Prostate Cancer in Vivo. *Nutr. Cancer* **2008**, *60*, 483–491. [CrossRef]
70. Wang, J.; Man, G.C.W.; Chan, T.H.; Kwong, J.; Wang, C.C. A Prodrug of Green Tea Polyphenol (-)-Epigallocatechin-3-Gallate (Pro-EGCG) Serves as a Novel Angiogenesis Inhibitor in Endometrial Cancer. *Cancer Lett.* **2018**, *412*, 10–20. [CrossRef]
71. Yang, Q.-Q.; Wei, X.-L.; Fang, Y.-P.; Gan, R.-Y.; Wang, M.; Ge, Y.-Y.; Zhang, D.; Cheng, L.-Z.; Corke, H. Nanochemoprevention with Therapeutic Benefits: An Updated Review Focused on Epigallocatechin Gallate Delivery. *Crit. Rev. Food Sci. Nutr.* **2020**, *60*, 1243–1264. [CrossRef]
72. Hamano, N.; Böttger, R.; Lee, S.E.; Yang, Y.; Kulkarni, J.A.; Ip, S.; Cullis, P.R.; Li, S.-D. Robust Microfluidic Technology and New Lipid Composition for Fabrication of Curcumin-Loaded Liposomes: Effect on the Anticancer Activity and Safety of Cisplatin. *Mol. Pharm.* **2019**, *16*, 3957–3967. [CrossRef]
73. Nocito, M.C.; De Luca, A.; Prestia, F.; Avena, P.; La Padula, D.; Zavaglia, L.; Sirianni, R.; Casaburi, I.; Puoci, F.; Chimento, A.; et al. Antitumoral Activities of Curcumin and Recent Advances to ImProve Its Oral Bioavailability. *Biomedicines* **2021**, *9*, 1476. [CrossRef]
74. Zheng, B.; McClements, D.J. Formulation of More Efficacious Curcumin Delivery Systems Using Colloid Science: Enhanced Solubility, Stability, and Bioavailability. *Molecules* **2020**, *25*, 2791. [CrossRef] [PubMed]
75. Konstantinov, S.M.; Kostovski, A.; Berger, M.R. Will Human Urinary Bladder Carcinoma Respond to Treatment with Alkylphosphocholines and Curcumin? *Facta Univ.* **2002**, *9*, 70–73.
76. Hauser, P.J.; Han, Z.; Sindhwani, P.; Hurst, R. Sensitivity of Bladder Cancer Cells to Curcumin and Its Derivatives Depends on the Extracellular Matrix. *Anticancer Res.* **2007**, *27*, 737–740. [PubMed]
77. Choi, H.Y.; Lim, J.E.; Hong, J.H. Curcumin interrupts the interaction between the androgen receptor and Wnt/β-catenin signaling pathway in LNCaP prostate cancer cells. *Prostate Cancer Prostatic Dis.* **2010**, *13*, 343–349. [CrossRef]
78. Eslami, S.S.; Jafari, D.; Montazeri, H.; Sadeghizadeh, M.; Tarighi, P. Combination of Curcumin and Metformin Inhibits Cell Growth and Induces Apoptosis without Affecting the Cell Cycle in LNCaP Prostate Cancer Cell Line. *Nutr. Cancer* **2020**, *73*, 1026–1039. [CrossRef] [PubMed]
79. Dhima, I.; Zerikiotis, S.; Lekkas, P.; Simos, Y.V.; Gkiouli, M.; Vezyraki, P.; Dounousi, E.; Ragos, V.; Giannakopoulos, X.; Baltogiannis, D.; et al. Curcumin Acts as a Chemosensitizer for Leiomyosarcoma Cells In Vitro But Fails to Mediate Antioxidant Enzyme Activity in Cisplatin-Induced Experimental Nephrotoxicity in Rats. *Integr. Cancer Ther.* **2019**, *18*. [CrossRef]
80. Muthoosamy, K.; Abubakar, I.B.; Bai, R.G.; Loh, H.-S.; Manickam, S. Exceedingly Higher co-loading of Curcumin and Paclitaxel onto Polymer-functionalized Reduced Graphene Oxide for Highly Potent Synergistic Anticancer Treatment. *Sci. Rep.* **2016**, *6*, 32808. [CrossRef]
81. Cianfruglia, L.; Minnelli, C.; Laudadio, E.; Scirè, A.; Armeni, T. Side Effects of Curcumin: Epigenetic and Antiproliferative Implications for Normal Dermal Fibroblast and Breast Cancer Cells. *Antioxidants* **2019**, *8*, 382. [CrossRef]
82. Shenouda, N.S.; Zhou, C.; Browning, J.D.; Ansell, P.J.; Sakla, M.S.; Lubahn, D.B.; Macdonald, R.S. Phytoestrogens in Common Herbs Regulate Prostate Cancer Cell Growth in Vitro. *Nutr. Cancer* **2004**, *49*, 200–208. [CrossRef]
83. Luo, K.-W.; Lung, W.-Y.; Xie, C.; Luo, X.-L.; Huang, W.-R. EGCG inhibited bladder cancer T24 and 5637 cell proliferation and migration via PI3K/AKT pathway. *Oncotarget* **2018**, *9*, 12261–12272. [CrossRef] [PubMed]
84. Sinjari, B.; Pizzicannella, J.; D'Aurora, M.; Zappacosta, R.; Gatta, V.; Fontana, A.; Trubiani, O.; Diomede, F. Curcumin/Liposome Nanotechnology as Delivery Platform for Anti-inflammatory Activities via NFkB/ERK/pERK Pathway in Human Dental Pulp Treated With 2-HydroxyEthyl MethAcrylate (HEMA). *Front. Physiol.* **2019**, *10*, 633. [CrossRef]

85. Mohammadi, S.S.; Vaezi, Z.; Shojaedin-Givi, B.; Naderi-Manesh, H. Chemiluminescent liposomes as a theranostic carrier for detection of tumor cells under oxidative stress. *Anal. Chim. Acta* **2019**, *1059*, 113–123. [CrossRef]
86. Verheijen, M.; Lienhard, M.; Schrooders, Y.; Clayton, O.; Nudischer, R.; Boerno, S.; Timmermann, B.; Selevsek, N.; Schlapbach, R.; Gmuender, H.; et al. DMSO induces drastic changes in human cellular processes and epigenetic landscape in vitro. *Sci. Rep.* **2019**, *9*, 4641. [CrossRef]
87. Galvao, J.; Davis, B.; Tilley, M.; Normando, E.; Duchen, M.R.; Cordeiro, M.F. Unexpected low-dose toxicity of the universal solvent DMSO. *FASEB J.* **2013**, *28*, 1317–1330. [CrossRef]
88. Rizeq, B.; Gupta, I.; Ilesanmi, J.; Alsafran, M.; Rahman, M.; Ouhtit, A. The Power of Phytochemicals Combination in Cancer Chemoprevention. *J. Cancer* **2020**, *11*, 4521–4533. [CrossRef] [PubMed]
89. Ghosh, A.K.; Kay, N.E.; Secreto, C.R.; Shanafelt, T.D. Curcumin Inhibits Prosurvival Pathways in Chronic Lymphocytic Leukemia B Cells and May Overcome Their Stromal Protection in Combination with EGCG. *Clin. Cancer Res.* **2009**, *15*, 1250–1258. [CrossRef] [PubMed]
90. La Barbera, G.; Capriotti, A.L.; Caracciolo, G.; Cavaliere, C.; Cerrato, A.; Montone, C.M.; Piovesana, S.; Pozzi, D.; Quagliarini, E.; Laganà, A. A comprehensive analysis of liposomal biomolecular corona upon human plasma incubation: The evolution towards the lipid corona. *Talanta* **2019**, *209*, 120487. [CrossRef] [PubMed]
91. Foteini, P.; Pippa, N.; Naziris, N.; Demetzos, C. Physicochemical study of the protein–liposome interactions: Influence of liposome composition and concentration on protein binding. *J. Liposome Res.* **2019**, *29*, 313–321. [CrossRef]
92. Pozzi, D.; Caracciolo, G.; Digiacomo, L.; Colapicchioni, V.; Palchetti, S.; Capriotti, A.L.; Cavaliere, C.; Chiozzi, R.Z.; Puglisi, A.; Laganà, A. The biomolecular corona of nanoparticles in circulating biological media. *Nanoscale* **2015**, *7*, 13958–13966. [CrossRef]
93. Roberts, S.A.; Lee, C.; Singh, S.; Agrawal, N. Versatile Encapsulation and Synthesis of Potent Therapeutic Liposomes by Thermal Equilibration. *bioRxiv* **2021**. [CrossRef]